

An Amide-Linked Chromophore–Catalyst Assembly for Water Oxidation

Dennis L. Ashford, David J. Stewart, Christopher R. Glasson, Robert A. Binstead, Daniel P. Harrison, Michael R. Norris, Javier J. Concepcion, Zhen Fang, Joseph L. Templeton, and Thomas J. Meyer*

Department of Chemistry, University of North Carolina at Chapel Hill, CB 3290, Chapel Hill, North Carolina 27599-3290, United States

Supporting Information

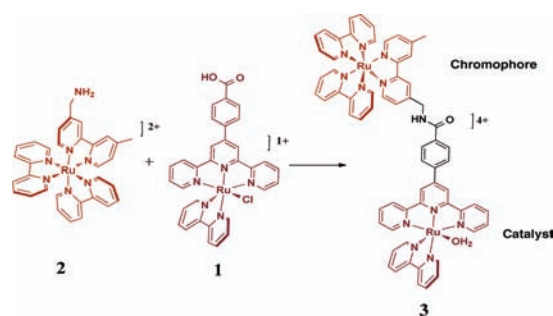
ABSTRACT: The synthesis and analysis of a new amide-linked, dinuclear $[\text{Ru}(\text{bpy})_2(\text{bpy-ph-NH-CO-trpy})\text{Ru}(\text{bpy})(\text{OH}_2)]^{4+}$ ($\text{bpy} = 2,2'$ -bipyridine; $\text{bpy-ph-NH-CO-trpy} = 4-(2,2':6',2''\text{-terpyridin-4'-yl})\text{-N}[(4'\text{-methyl-2,2'-bipyridin-4-yl)methyl]benzamide$) assembly that incorporates both a light-harvesting chromophore and a water oxidation catalyst are described. With the saturated methylene linker present, the individual properties of both the chromophore and catalyst are retained including water oxidation catalysis and relatively slow energy transfer from the chromophore excited state to the catalyst.

In producing solar fuels from artificial photosynthesis, as in natural photosynthesis, integrating visible-light absorption with the sequential redox events that drive the coupled half-reactions—water oxidation to oxygen and either water/ H^+ reduction to hydrogen or CO_2 reduction to CO , other oxygenates, or hydrocarbons—is an essential element.¹ The use of “chromophore–catalyst assemblies”, which combine both light absorption and catalysis in linked molecular units bound to large-band-gap semiconductors, is appealing for use in dye-sensitized photoelectrosynthesis cells.²

Catalytic water oxidation has been demonstrated for assemblies that incorporate both a light-absorbing chromophore and a water oxidation catalyst.^{3a} Excitation and injection into TiO_2 was recently reported for a surface anchored assembly; however, electron-injection efficiencies were low because of electron trapping by a lowest-lying metal-to-ligand charge transfer (MLCT) state localized on the π^* system of the bridging ligand.^{3b}

We report here the development of a general synthetic approach to chromophore–catalyst assemblies based on amide coupling that produces chemically linked chromophore–catalyst units free of complications from the photophysical or redox properties of the intervening bridge. In this strategy, the water oxidation catalyst precursor $[\text{Ru}[4-(2,2':6',2''\text{-terpyridin-4'-yl})\text{benzoic acid}](\text{bpy})(\text{Cl})]^+$ (**1**) and the chromophore $[\text{Ru}(\text{bpy})_2(4'\text{-methyl-2,2'-bipyridin-4-yl})\text{methanamine}]^{2+}$ (**2**) were used as starting materials for synthesis of the assembly $[(\text{Ru}(\text{bpy})_2(\text{bpy-ph-NH-CO-trpy})\text{Ru}(\text{bpy})(\text{OH}_2))]^{4+}$ ($\text{bpy-ph-NH-CO-trpy} = 4-(2,2':6',2''\text{-terpyridin-4'-yl})\text{-N}[(4'\text{-methyl-2,2'-bipyridin-4-yl})\text{methyl}]benzamide$) (**3**; Scheme 1). The flexibility of amide coupling provides a general approach to a family of chromophore–catalyst assemblies that can be

Scheme 1. Amide-Coupling Strategy Used To Prepare the Chromophore–Catalyst Assembly



configured with different bridge lengths and intervening spacers. The syntheses of both the water oxidation catalyst and chromophore use straightforward, high-yield reactions, without requiring chromatographic separation (see the Supporting Information, SI). In the resulting assembly, the properties of the constituent units, including water oxidation catalysis, are retained.⁴

Unlike amide couplings utilizing acid chloride/amine reactions, which are typically carried out at or below room temperature, formation of the amide link between complexes requires elevated temperatures to proceed at reasonable rates because of the decreased nucleophilicity of the coordinated $(4'\text{-methyl-2,2'-bipyridin-4-yl})\text{methanamine}$ (**8**) ligand.⁵ This hypothesis is supported by control experiments: (i) the acid chloride derivative of **1** was shown to react with **8** in N,N -dimethylformamide (DMF) in the presence of N,N -diisopropylethylamine (DIPEA) at room temperature with complete conversion (by NMR); (ii) by contrast, **2** does not react with benzoyl chloride or the acid chloride of $4-(2,2':6',2''\text{-terpyridin-4'-yl})\text{benzoic acid}$ (**4**) in DMF with DIPEA at $40\text{ }^\circ\text{C}$; (iii) both of these reactions proceed to completion at $100\text{ }^\circ\text{C}$.

The methylene-based amide bridge between ligands provides a saturated link between the two metal complexes, resulting in retention of the spectral and redox properties of the constituents. In the UV–vis absorption spectrum of **3**, a MLCT absorption appears at $\lambda_{\text{max}} \sim 460\text{ nm}$ arising from overlapping MLCT absorptions of both the chromophore and catalyst (Figure S4 in the SI). The spectrum is the sum of the

Received: January 10, 2012

Published: June 1, 2012

constituents, as shown in Figure 1. The high molar absorptivity of the MLCT band for **3** ($26000 \text{ M}^{-1} \text{ cm}^{-1}$) is near the sum of

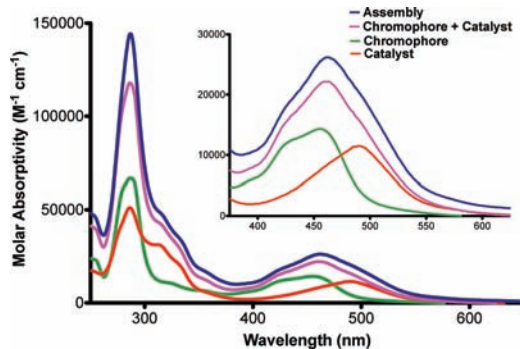


Figure 1. Normalized UV-vis absorption spectra of **9** (red), **10** (green), **9 + 10** (pink), and **3** (blue).

the component MLCT extinction coefficients, $11500 \text{ M}^{-1} \text{ cm}^{-1}$ for $[\text{Ru}[4-(2,2':6',2''\text{-terpyridin-4'-yl)benzoic acid}](\text{bpy})-(\text{OH}_2)]^{2+}$ (**9**) and $14300 \text{ M}^{-1} \text{ cm}^{-1}$ for $[\text{Ru}(\text{bpy})_2(4,4'\text{-dimethyl-2,2'-bipyridine})]^{2+}$ (**10**; Figures S5 and S6 in the SI).⁶ Consistent with deprotonation of $-\text{Ru}^{\text{II}}-\text{OH}_2^{2+}$ ($\text{p}K_{\text{a}} = 10.0$), a red shift in the spectrum occurs upon an increase in the pH to ~ 13 (Figure S4 in the SI).

Cyclic voltammograms of **3** at pH 2.1 include waves for the expected $\text{Ru}^{\text{II}}-\text{Ru}^{\text{III}}-\text{OH}/\text{Ru}^{\text{II}}-\text{Ru}^{\text{II}}-\text{OH}_2$, $\text{Ru}^{\text{II}}-\text{Ru}^{\text{IV}}=\text{O}/\text{Ru}^{\text{II}}-\text{Ru}^{\text{III}}-\text{OH}$, and $\text{Ru}^{\text{III}}-\text{Ru}^{\text{IV}}=\text{O}/\text{Ru}^{\text{II}}-\text{Ru}^{\text{IV}}=\text{O}$ couples at $E_{1/2} = 1.01, 1.11,$ and 1.22 V (vs NHE), respectively (Figure 2). As for the related monomer, $\text{Ru}(\text{trpy})(\text{bpy})(\text{OH}_2)^{2+}$, the

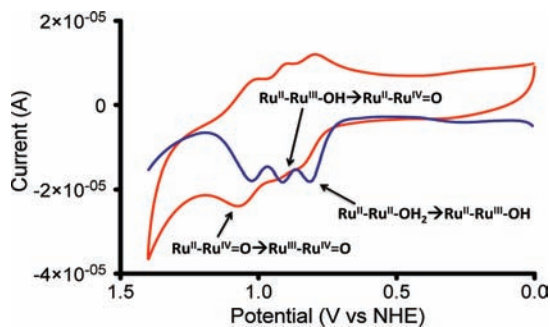


Figure 2. Cyclic voltammogram of **3** at pH 2.1 ($0.05 \text{ M H}_2\text{PO}_4$, $0.05 \text{ M H}_3\text{PO}_4$ phosphate, and 0.5 M KNO_3) at 100 mV s^{-1} with a glassy carbon working electrode (0.07 cm^2 , red) and a differential pulse voltammogram of **3** (blue) at $298 \pm 3 \text{ K}$.

first two are pH-dependent, with the results summarized in the $E_{1/2}$ ($\sim E^{\circ}$: E° is the formal potential) versus pH (Pourbaix) diagram in Figure S11 in the SI.⁷

A summary of the $E_{1/2}$ -pH results follows: (i) Both $-\text{Ru}^{\text{III}}/\text{II}$ and $-\text{Ru}^{\text{IV}}/\text{III}$ couples are pH-dependent because of acid-base equilibria for $-\text{Ru}^{\text{III}}-\text{OH}_2^{3+}$ ($\text{p}K_{\text{a},1} = 1.0$) and $-\text{Ru}^{\text{II}}-\text{OH}_2^{2+}$ ($\text{p}K_{\text{a},1} = 10.0$). $E_{1/2}$ values are 1.05 V for the $-\text{Ru}^{\text{III}}-\text{OH}_2^{3+}/-\text{Ru}^{\text{II}}-\text{OH}_2^{2+}$ couple and 1.17 V for the $-\text{Ru}^{\text{IV}}=\text{O}^{2+}/-\text{Ru}^{\text{III}}-\text{OH}_2^{3+}$ couple in 0.1 M HNO_3 . By comparison, for $\text{Ru}(\text{tpy})(\text{bpy})(\text{OH}_2)^{2+}$, the corresponding values are 1.04 V for $\text{Ru}^{\text{III}}-\text{OH}_2^{3+}/\text{Ru}^{\text{II}}-\text{OH}_2^{2+}$ and 1.15 V for $\text{Ru}^{\text{IV}}=\text{O}^{2+}/\text{Ru}^{\text{III}}-\text{OH}_2^{3+}$.⁷ (ii) Below pH 1.0, $E_{1/2}$ for the $-\text{Ru}^{\text{IV}}=\text{O}^{2+}/-\text{Ru}^{\text{III}}-\text{OH}_2^{3+}$ couple increases by 120 mV/pH unit, consistent with a $1\text{e}^-/2\text{H}^+$ couple. Above pH 0.5, $E^{\circ}(\text{Ru}^{\text{III}}/\text{II}) > E^{\circ}(-\text{Ru}^{\text{IV}}=\text{O}^{2+}/-\text{Ru}^{\text{III}}-\text{OH}_2^{3+})$ and the $\text{Ru}^{\text{III}}/\text{II}$ couple at the chromophore is a

sufficient oxidant to oxidize the aqua complex from $-\text{Ru}^{\text{III}}-\text{OH}_2^{3+}$ to $-\text{Ru}^{\text{IV}}=\text{O}^{2+}$. (iii) At pH 11.0, the variation in $E_{1/2}$ with pH becomes $\sim 30 \text{ mV/pH}$ unit, consistent with the $2\text{e}^-/1\text{H}^+$ couple $-\text{Ru}^{\text{IV}}=\text{O}^{2+}/-\text{Ru}^{\text{II}}-\text{OH}^+$. As the pH is increased above 11.0, $E^{\circ}(-\text{Ru}^{\text{III}}-\text{OH}_2^{3+}) > E^{\circ}(-\text{Ru}^{\text{IV}}=\text{O}^{2+}/-\text{Ru}^{\text{III}}-\text{OH}_2^{3+})$ and $-\text{Ru}^{\text{III}}-\text{OH}_2^{3+}$ is unstable with respect to disproportionation into $-\text{Ru}^{\text{IV}}=\text{O}^{2+}$ and $-\text{Ru}^{\text{II}}-\text{OH}^+$. (iv) Oxidation of the chromophore is pH-independent and occurs at $E_{1/2}(\text{Ru}^{\text{III}}/\text{II}) = 1.23 \text{ V}$. Notably, within experimental error, the potential for oxidation of the chromophore is independent of whether the catalyst is $-\text{Ru}^{\text{III}}-\text{OH}_2^{3+}$ or $-\text{Ru}^{\text{IV}}=\text{O}^{2+}$. This observation is consistent with minimal interactions across the bridge between the complexes. E° values are slightly more positive than those for the constituent complexes because of the higher overall charge on the assembly (see Figure S3 in the SI).

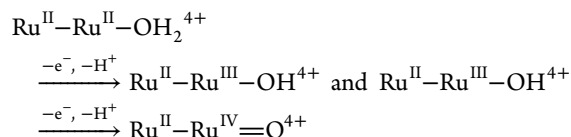
In water, the expected $\text{Ru}^{\text{III}}-\text{Ru}^{\text{V}}=\text{O}^{3+}/\text{Ru}^{\text{III}}-\text{Ru}^{\text{IV}}=\text{O}^{2+}$ couple was not observable because of the onset of water oxidation at $\sim 1.6 \text{ V}$ (Figure 2). Oxidation of **3** was investigated by differential pulse voltammetry in 2% water-propylene carbonate (PC; v/v) mixtures to minimize water oxidation.⁸ These measurements reveal an additional wave for the expected $-\text{Ru}^{\text{V}}=\text{O}^{3+}/-\text{Ru}^{\text{IV}}=\text{O}^{2+}$ couple at $E_{\text{p,a}} \sim 1.87 \text{ V}$ ($E_{\text{p,a}}$ is the anodic peak potential) relative to the $(\text{Ru}^{\text{III}}/\text{II})^{3+/2+}-\text{Ru}^{\text{IV}}=\text{O}$ wave at $E_{1/2} = 1.23 \text{ V}$; Table 1 and Figure S1 in the SI.

Table 1. Summary of the Electrochemical Properties

complex	$E_{1/2}$ (V vs NHE) ^a			chrom. $\text{Ru}^{\text{III}}/\text{II}$	$\text{p}K_{\text{a}}^c$	
	cat. $\text{Ru}^{\text{II}}/\text{III}$	cat. $\text{Ru}^{\text{III}}/\text{IV}$	cat. $\text{Ru}^{\text{IV}}/\text{V}$		$\text{Ru}^{\text{II}}-\text{OH}_2$	$\text{Ru}^{\text{III}}-\text{OH}_2$
3	0.95	1.04	$\sim 1.87^b$	1.23	10.0	1.0
9	0.93	1.03	~ 1.80		10.5^d	1.7^d
10 ^e				1.17		

^aIn pH 3.1 ($0.43 \text{ M H}_2\text{PO}_4$, $0.07 \text{ M H}_3\text{PO}_4$, and 0.5 M KNO_3) at $23 \text{ }^\circ\text{C}$ from differential pulse voltammetry peak currents at glassy carbon (0.07 cm^2) with platinum counter electrode, vs the Ag/AgCl reference electrode (0.197 V vs NHE). ^bIn 2% water-PC; see the text. ^cFrom pH-dependent electrochemical measurements (Figure 2). ^dData for $\text{Ru}(\text{tpy})(\text{bpy})(\text{OH}_2)^{2+}$. ^e $\text{Ru}(\text{bpy})_2(4,4'\text{-Me}_2\text{bpy})^{2+}$.

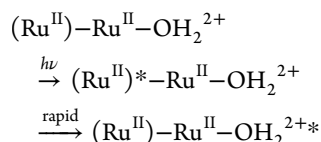
As noted in Figures 2 and S8 in the SI, there is clear evidence for catalytic water oxidation with an onset at $\sim 1.6 \text{ V}$. The ability of **3** to act as a catalyst for net Ce^{IV} oxidation of water, $4\text{Ce}^{\text{IV}} + 2\text{H}_2\text{O} \rightarrow 4\text{Ce}^{\text{III}} + \text{O}_2 + 4\text{H}^+$, was investigated by a series of mixing experiments. In these experiments, 30 equiv of Ce^{IV} in 1.0 M HNO_3 was added to **3** (Figure S12 in the SI). The addition of Ce^{IV} resulted in the immediate loss of MLCT absorption of the chromophore with its reappearance upon complete consumption of Ce^{IV} . Evolved oxygen was monitored by gas chromatography, giving a yield of $\sim 70\%$ O_2 based on Ce^{IV} added (see the SI). Although not studied in detail, as for related single-site ruthenium catalysts,⁷ water oxidation occurs by oxidative activation by proton-coupled electron transfer



followed by two single-electron oxidations to $\text{Ru}^{\text{III}}-\text{Ru}^{\text{V}}=\text{O}^{6+}$ and water attack on the electrophilic O atom with proton transfer to a second water molecule by atom-proton transfer (Figure S8 in the SI).⁹

The reversibility of the $-\text{Ru}^{\text{IV}}=\text{O}^{2+}/-\text{Ru}^{\text{III}}-\text{OH}^{2+}$ couple (Figure 2) provides evidence for a kinetic contribution by the chromophore as a redox mediator in water oxidation. This behavior is in marked contrast to the analogous $\text{Ru}(\text{trpy})(\text{bpy})(\text{O})^{2+}/\text{Ru}(\text{trpy})(\text{bpy})(\text{OH})^{3+}$ couple, which is kinetically slow at inert electrodes.⁷ Another observation is the appearance of an onset for water oxidation at ~ 1.6 V, well below $E_{\text{pa}} \sim 1.87$ V for the $-\text{Ru}^{\text{V}}(\text{O})^{3+}/-\text{Ru}^{\text{IV}}(\text{O})^{2+}$ couple and the catalytic onset of ~ 1.7 – 1.8 V for water oxidation by $\text{Ru}(\text{tpy})(\text{bpy})(\text{OH}_2)^{2+}$.⁷ Related electron-transfer mediator effects have been observed for the $\text{Ru}(\text{bpy})_3^{2+}$ couple because of its nearly barrierless rate of self-exchange.^{2a,9d} Mediator effects exist because of diminished reorganization energy barriers at the interface. Rates for mediated pathways are dictated by the magnitude of ΔG for the electron-transfer step and the reorganization energy for the following reaction.

Preliminary transient absorption and emission results in argon-deaerated deionized water at room temperature provide evidence for intraassembly energy transfer. MLCT excitation (445 nm) of $\text{Ru}(\text{trpy})(\text{bpy})(\text{OH}_2)^{2+}$ results in no observable transient on the 15 ns time scale by absorption monitoring. Emission is observed following excitation of **2** with $\tau = 568$ ns. As monitored by transient absorption and emission measurements, excitation of **3** (445 nm) results in biphasic kinetics with $\tau_1 = 18$ and $\tau_2 = 410$ ns ($k_1 = 5 \times 10^7 \text{ s}^{-1}$; $k_2 = 2.4 \times 10^6 \text{ s}^{-1}$); see the SI. These observations are qualitatively consistent with excitation at the chromophore followed by intraassembly energy transfer



and rapid decay to $-\text{Ru}^{\text{II}}-\text{OH}_2$ in competition with emission from the excited state of the chromophore $(\text{Ru}^{\text{II}})^*-\text{Ru}^{\text{II}}-\text{OH}_2^{2+} \rightarrow (\text{Ru}^{\text{II}})-\text{Ru}^{\text{II}}-\text{OH}_2^{2+}$.^{9e} This time scale is relatively slow compared to the far faster typical subpicosecond rates of injection into TiO_2 for surface-bound analogues. Experiments are currently underway to examine in more detail the photophysical properties of the assembly and its oxidized forms.

We have demonstrated here a versatile approach for preparing chromophore–catalyst assemblies based on amide couplings between preformed complexes. This route offers synthetic generality and flexibility in the nature of the chromophore, catalyst, and connecting link. The individual properties of the constituents are retained, allowing for optimization of the properties of the separate components before being placed into an assembly by application of the “modular approach”.^{1b,c,3a,b}

■ ASSOCIATED CONTENT

● Supporting Information

Detailed experimental procedures and electrochemical, kinetic, photophysical, and oxygen measurement analysis. This material is available free of charge via the Internet at <http://pubs.acs.org>.

■ AUTHOR INFORMATION

Corresponding Author

*E-mail: tjmeyer@unc.edu.

Notes

The authors declare no competing financial interest.

■ ACKNOWLEDGMENTS

This work was funded by the UNC EFRC “Center for Solar Fuels”, an EFRC funded by the U.S. Department of Energy, Office of Science, Office of Basic Energy Sciences, under Award DE-SC0001011 supporting D.L.A., R.A.B., D.P.H., M.R.N., and Z.F. (T.J.M., J.L.T., J.J.C.). We acknowledge an Army Research Office Award W911NF-09-1-0426 supporting CRG (T.J.M.) and NSF Grant CHE-0957215 supporting D.J.S. (T.J.M.). We acknowledge support for the purchase of instrumentation from the UNC EFRC (DOE Award DE-SC0001011 as above) and UNC SERC (“Solar Energy Research Center Instrumentation Facility” funded by US DOE Office of Energy Efficiency & Renewable Energy Award DE-EE0003188).

■ REFERENCES

- (1) (a) Lewis, N. S.; Nocera, D. G. *Proc. Natl. Acad. Sci. U.S.A.* **2006**, *103*, 15729–15735. (b) Concepcion, J. J.; Jurss, J. W.; Brennaman, M. K.; Hoertz, P. G.; Patrocinio, A. O. T.; Murakami Iha, N. Y.; Templeton, J. L.; Meyer, T. J. *Acc. Chem. Res.* **2009**, *42*, 1954–1965. (c) Alstrum-Acevedo, J. H.; Brennaman, M. K.; Meyer, T. J. *Inorg. Chem.* **2005**, *44*, 6802–6827. (d) Concepcion, J. J.; Jurss, J. W.; Templeton, J. L.; Meyer, T. J. *J. Am. Chem. Soc.* **2008**, *130*, 16462–16463.
- (2) (a) Concepcion, J. J.; Jurss, J. W.; Templeton, J. L.; Meyer, T. J. *Proc. Natl. Acad. Sci. U.S.A.* **2008**, *105*, 17632–17635. (b) Treadway, J. A.; Moss, J. A.; Meyer, T. J. *Inorg. Chem.* **1999**, *38*, 4386–4387. (c) Li, F.; Jiang, Y.; Zhang, B.; Huang, F.; Gao, Y.; Sun, L. *Angew. Chem., Int. Ed.* **2012**, *51*, 2417–2420.
- (3) (a) Concepcion, J. J.; Jurss, J. W.; Hoertz, P. G.; Meyer, T. J. *Angew. Chem., Int. Ed.* **2009**, *48*, 9473–9476. (b) Song, W.; Glasson, C. R. K.; Luo, H.; Hanson, K.; Brennaman, M. K.; Concepcion, J. J.; Meyer, T. J. *J. Phys. Chem. Lett.* **2011**, *2*, 1808–1813.
- (4) (a) Brennaman, M. K.; Patrocinio, A. O. T.; Song, W.; Jurss, J. W.; Concepcion, J. J.; Hoertz, P. G.; Traub, M. C.; Murakami Iha, N. Y.; Meyer, T. J. *ChemSusChem* **2011**, *4*, 216–227. (b) Galoppini, E.; Guo, W.; Zhang, W.; Hoertz, P. G.; Qu, P.; Meyer, G. J. *J. Am. Chem. Soc.* **2002**, *124*, 7801–7811.
- (5) (a) Ozawa, H.; Sakai, K. *Chem. Lett.* **2007**, *36*, 920–921. (b) Uemura, K.; Kumamoto, Y.; Kitagawa, S. *Chem.—Eur. J.* **2008**, *14*, 9565–9576.
- (6) McClanahan, S. F.; Dallinger, R. F.; Holler, F. J.; Kincaid, J. R. *J. Am. Chem. Soc.* **1985**, *107*, 4853–4860.
- (7) (a) Takeuchi, K. J.; Thompson, M. S.; Pipes, D. W.; Meyer, T. J. *Inorg. Chem.* **1984**, *23*, 1845–1851. (b) Wasylenko, D. J.; Ganesamoorthy, C.; Henderson, M. A.; Koivisto, B. D.; Osthoff, H. D.; Berlinguette, C. P. *J. Am. Chem. Soc.* **2010**, *132*, 16094–16106. (c) Wasylenko, D. J.; Ganesamoorthy, C.; Henderson, M. A.; Berlinguette, C. P. *Inorg. Chem.* **2011**, *50*, 3662–3672. (d) Yoshida, M.; Masaoka, S.; Sakai, K. *Chem. Lett.* **2009**, *38*, 702–703.
- (8) Chen, Z.; Concepcion, J. J.; Luo, H.; Hull, J. F.; Paul, A.; Meyer, T. J. *J. Am. Chem. Soc.* **2010**, *132*, 17670–17673.
- (9) (a) Chen, Z.; Concepcion, J. J.; Hu, X.; Yang, W.; Hoertz, P. G.; Meyer, T. J. *Proc. Natl. Acad. Sci. U.S.A.* **2010**, *107*, 7225–7229. (b) Concepcion, J. J.; Tsai, M.-K.; Muckerman, J. T.; Meyer, T. J. *J. Am. Chem. Soc.* **2010**, *132*, 1545. (c) Hughes, T. F.; Friesner, R. A. *J. Phys. Chem. B* **2011**, *115*, 9280–9289. (d) Young, R. C.; Keene, F. R.; Meyer, T. J. *J. Am. Chem. Soc.* **1977**, *99*, 2468–2473. (e) Thompson, D. W.; Fleming, C. N.; Myron, B. D.; Meyer, T. J. *J. Phys. Chem. B* **2007**, *111*, 6930–6941.